Current Chemistry Letters 3 (2014) 85–96

Contents lists available at Growing Science

Current Chemistry Letters

homepage: www.GrowingScience.com/ccl

X-Ray, IR, NMR, UV-visible spectra and DFT analysis of 5-aryloxy-(1*H*)-tetrazoles, structure, conformation and tautomerism

Nader Noroozi Pesyan[a*], Sadeghali Bavafa[b], Mohammad Samim Enayati[a], Sajedin Hoseinpour[c], Narges Ostadhosseini[a], Alireza Dadrass[a], Jannet Soleimannejad[d], Ertan Şahin[e] and Mohamed I. Mohamed Tahir[f]

[a]*Faculty of Chemistry, Urmia University, 57159, Urmia, Iran*
[b]*International University of Chabahar (IUC), Chabahar, Iran*
[c]*Department of Physical Chemistry, Faculty of Chemistry, University of Kashan, Kashan, Iran.*
[d]*Department of Chemistry, Faculty of Science, Tehran University, Tehran, Iran*
[e]*Department of Chemistry, Faculty of Science, Atatürk University, 25240, Erzurum, Turkey*
[f]*Department of Chemistry, Faculty of Science, Universiti Putra Malaysia, 43400 UPM Serdang, Selangor, Malaysia*

C H R O N I C L E

Article history:
Received June 28, 2013
Received in Revised form
December 10, 2013
Accepted 20 December 2013
Available online
21 December 2013

Keywords:
NMR; X-ray
Rotation barrier
H-bond
DFT
5-(2,6-Diisopropylphenoxy)-(1H-(tetrazole

A B S T R A C T

The predominant tautomeric forms of N1–H, N2–H of 5-(2,6-dimethyl- and 5-(2,6-diisopropylphenoxy)-(1*H*)-tetrazoles were analyzed at B3LYP method using 6-311G(d,p) basis set in the gas phase. The N1–H form of tetrazoles was found to be more stable than N2–H form in both solid and gas phases. Crystal structures of both tetrazoles show an intermolecular H-bond between N1-H and N4 atom of other tetrazole space. The hydrogen bonds between each tautomer of tetrazoles were evaluated at B3LYP/6-311G(d,p) level. The geometrical parameters and spectral data of tetrazoles and their variation were studied in both solid and gas phases.

1. Introduction

5-Substituted tetrazoles are reported to possess antibacterial[1], antifungal[2], antiviral [3], analgesic[4,5], anti-inflammatory[6], antiulcer[7] and antihypertensive[8] activities. The tetrazole function is metabolically stable [9]. The similarities between the acidic character of the tetrazole group and carboxylic acid group[10] have inspired medicinal chemists to synthesize substituted tetrazoles as potential medicinal agents. Tetrazoles are an important functionality, not only as precursors to a variety of nitrogen-containing heterocycles[11] but also as materials with applications in explosives[12] and even as

* Corresponding author. Tel.: (+98) 441 2972147, Fax: (+98) 441 2776707
E-mail addresses: n.noroozi@urmia.ac.ir (N. Noroozi Pesyan)

doi: 10.5267/j.ccl.2014.1.001

increasive lubricants[13]. Several works were reported about tetrazole tautomerization[14-16] and isomerization[17].

In this work, characteristics of geometrical parameters, harmonic frequencies and NMR that exist in complexes are completely investigated by a DFT (B3LYP) approach. Based on these concepts, as part of investigation of 5-(2,6-dimethyl- (**1**) and 5-(2,6-diisopropylphenoxy)-(1*H*)-tetrazole (**2**), herein we report the optimized structures of **1** and **2** in the gas and solid phases and also the corresponding experimental and optimized IR, ^{1}H NMR, ^{13}C NMR and UV-visible spectra in the solution and gas phases, respectively.

2. Results and Discussion

This paper presents results on the tautomeric behavior, rotation barrier and the comparison of the experimental and theoretical IR, ^{1}H, ^{13}C NMR and UV-visible spectra of 5-(2,6-dimethyl- **1** and 5-(2,6-diisopropylphenoxy)-(1*H*)-tetrazole **2** in both solution and gas phases. In this work, the experimental X-ray crystallographic data is also compared with calculated data. The ORTEP plot, crystal packing diagrams and formula structures of **1** and **2** are shown in **Figs. 1-4**, respectively. Possible tautomeric forms of 5-aryloxy tetrazoles and also tautomeric and rotameric forms of **1** and **2** are shown in **Schemes 1** and **2**, respectively. The optimized molecular structures of these compounds were calculated by B3LYP/6-311G(d,p) method and are shown in **Fig. 5**.

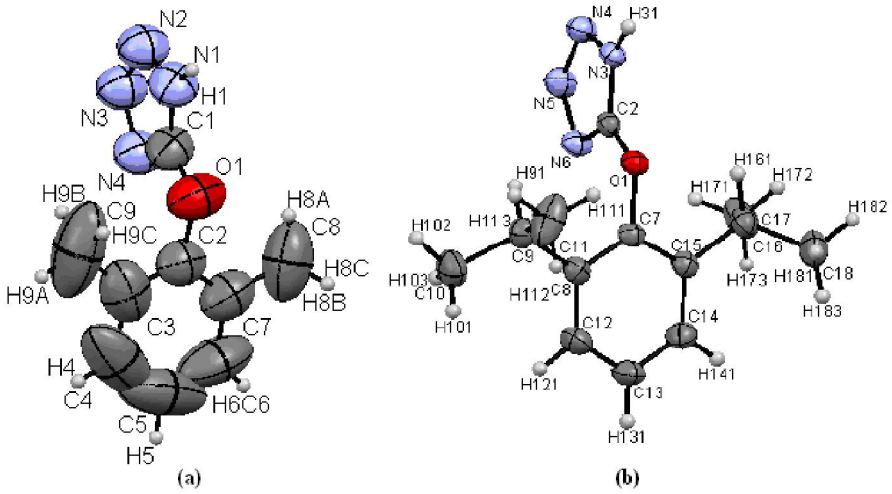

Fig. 1. Molecular structure of **1** (a) and **2** (b) with thermal ellipsoids drawn at 50%

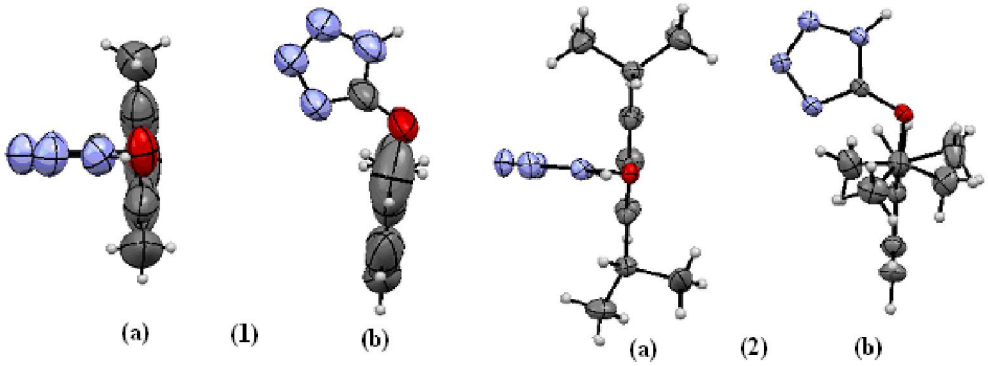

Fig. 2. Molecular structure of **1** and **2** viewed from top (a) and from edge (b)

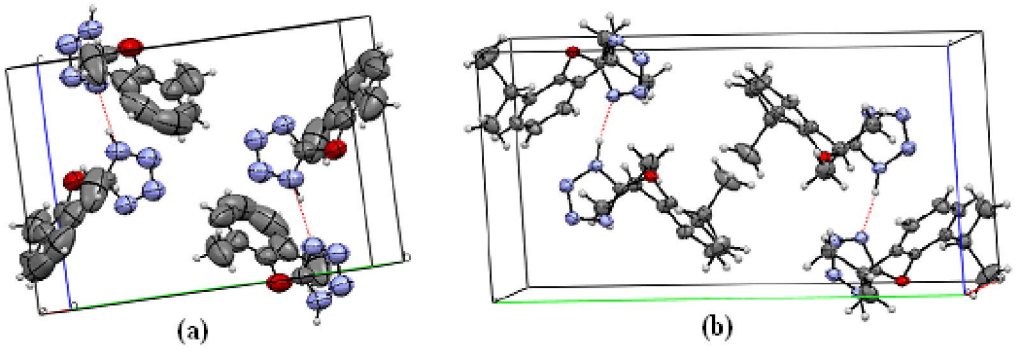

Fig. 3. The crystal packing diagram of **1** (a) and **2** (b)

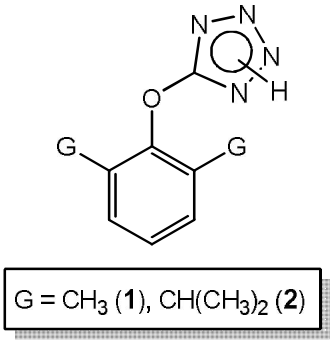

Fig. 4. The general formula structures of tetrazoles **1** and **2**

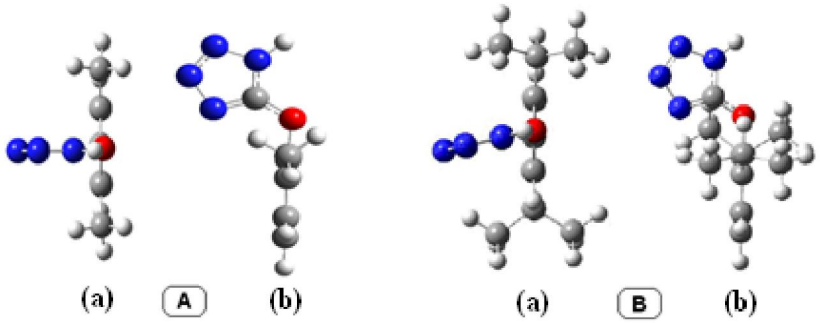

Fig. 5. Optimized molecular structures viewed from top (a) and edge (b) of **1** (**A**) and **2** (**B**), calculated at B3LYP/6-311G(d,p)

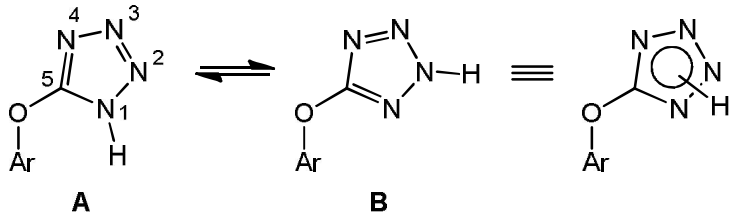

Scheme 1. Two possible tautomeric forms of tetrazole ring in 5-aryloxy tetrazoles [14]

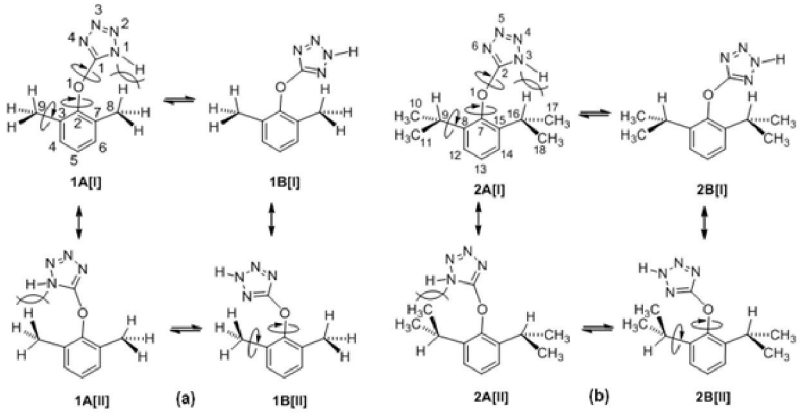

Scheme 2. Tautomeric forms and rotational barrier in tetrazoles **1** (a) and **2** (b) in both solid and gas phases (Atom numbering is based on crystal structure)

In the compound **1**, the crystal structure indicated that the tetrazole and phenyl rings are nearly perpendicular to each other, forming a dihedral angle of 95.5° (*versus* 92.08° from calcd. B3LYP/6-311G(d,p)). Because of the conjugation of O1 with tetrazole ring, the bond distance C1–O1 [1.322 Å] is slightly shorter than O1–C2 [1.399 Å]. These bond distances for C1–O1 and O1–C2 were obtained 1.330 and 1.419 Å with calculation by B3LYP/6-311G(d,p) method, respectively. These data are in good agreement with experimental results (**Table 2**). Similarly, in the compound **2**, the crystal structure indicated that the tetrazole and phenyl rings are nearly perpendicular to each other, forming a dihedral angle of 85.91° (*versus* 107.3° from calcd. B3LYP/6-311G(d,p)). Because of the conjugation of O1 with tetrazole ring, the bond distance C2–O1 [1.327 Å] is slightly shorter than O1–C7 [1.426 Å]. These bond distances for C2–O1 and O1–C7 were obtained 1.329 and 1.422 Å with calculation by B3LYP/6-311G(d,p) method, respectively and are in good agreement with experimental results. The torsion angles between phenyl ring and each of methyl units on two isopropyl groups are -110.70°, 124.18° and -80.2° and 154.12°, respectively (**Table 2**).The selected parameters of bond lengths, angles and torsion angles of **1** and **2** derived by experimental and calculated results are shown in **Table 2**. The crystal packing diagram of **1** exhibits an intermolecular N1–H1····N4 hydrogen bonds and compared with the calculated at B3LYP/6-311G(d,p) method (**Table 3**). The crystal structure indicated that the bond distance value between donor – hydrogen (N1–H1) and hydrogen-acceptor (H1····N4) were found in results 0.861 and 1.959 Å, respectively. For instance, these bond distances were also found in results 1.015 for (N1–H1) and 1.863 Å for (H1····N4) by calculated at B3LYP/6-311G(d,p) method. The donor-acceptor distance value (N1····N4) was obtained 2.804 by experimental method. This parameter was found 2.869 Å by B3LYP/6-311G(d,p) method. The angle of N1–H1····N4 was found 166.9 and 170.7° by experimental and calculated at B3LYP/6-31G(d), respectively. The results of calculated method are in good agreement with experimental results (**Table 3**). The crystal packing diagram of **2** also exhibits an intermolecular N3–H31····N6 hydrogen bonds with the calculated by B3LYP/6-311G(d,p) method (**Table 3**). The crystal structure indicated that the bond distance value between donor – hydrogen (N3–H31) and hydrogen acceptor (H31····N6) were found in results 0.926 and 1.919 Å, respectively. For instance, these bond distances were also found in results 1.009 for (N3–H31) and 1.938 Å for (H31····N6) by calculated at B3LYP/6-311G(d,p) method. The donor-acceptor distance value (N3····N6) was obtained 2.835 by experimental method. This parameter was found 2.940 Å by calculated methods B3LYP/6-311G(d,p) level. The angle of N3–H31····N6 was found 169.1 and 171.46° found by experimental and calculated at B3LYP/6-311G(d,p) method, respectively. The results of calculated method are in good agreement with experimental results (**Table 3**). The calculated structures for **1** and **2** having intermolecular H-bond are shown in **Fig. 6**.

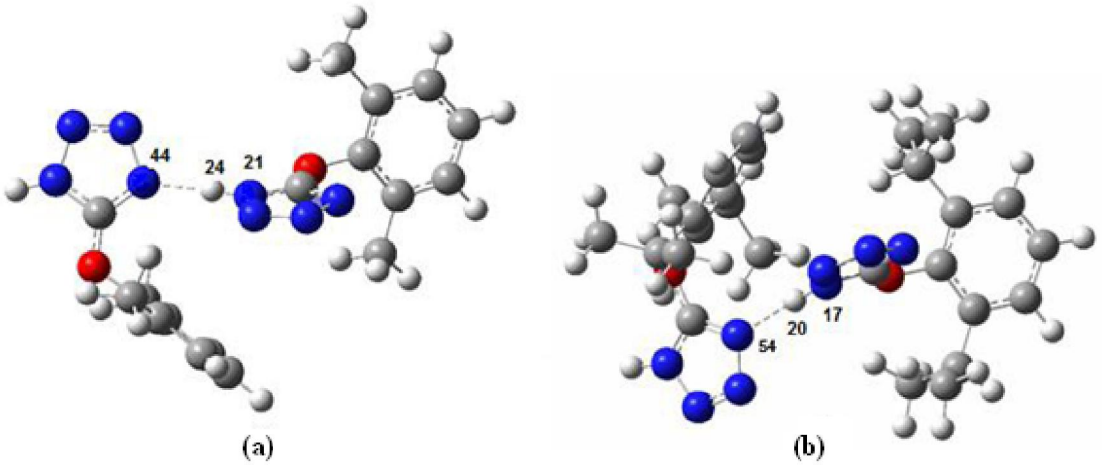

Fig. 6. Optimized structure and intermolecular H-bond in **1** (a) and **2** (b). Calculated at B3LYP/6-311 G(d,p) basis sets

IR spectra of **1** and **2** were derived from experimental and calculated results with B3LYP/6-311G(d,p) are shown in **Fig. 7** and **Fig. 8**, respectively. These data indicated the good agreement together between the experimental and calculated result (**Fig. 8**). ^{1}H and ^{13}C NMR spectra of **1** and **2** calculated at B3LYP/6-311G(d,p) method are also in good agreement with experimental results (**Figs. 9-10**). The UV-visible spectra of compounds **1** and **2** were measured in EtOH and the corresponding λ_{max} were obtained 335 nm for **1** and 297 and 354 nm for **2**, respectively (**Fig. 11**). UV-visible spectra of **1** and **2** were also calculated at B3LYP/6-311G(d,p) method and is shown in **Fig. 12**.

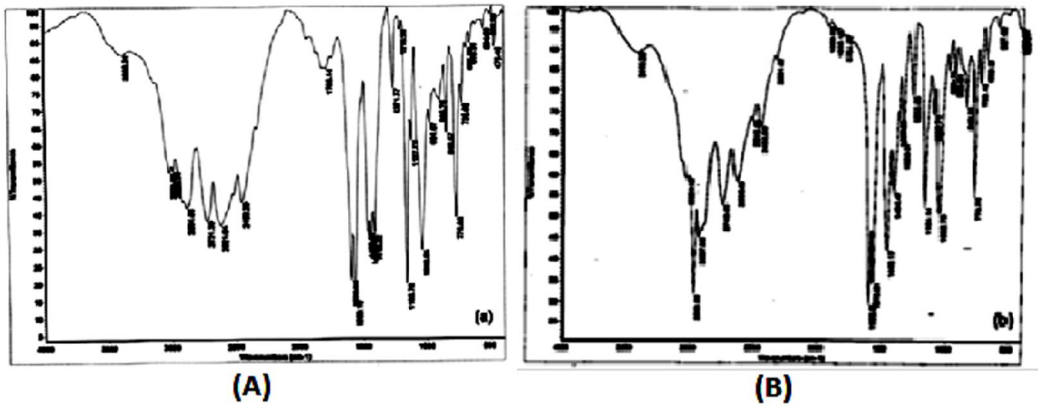

Fig. 7. IR spectra of **1** (A) and **2** (B) in KBr

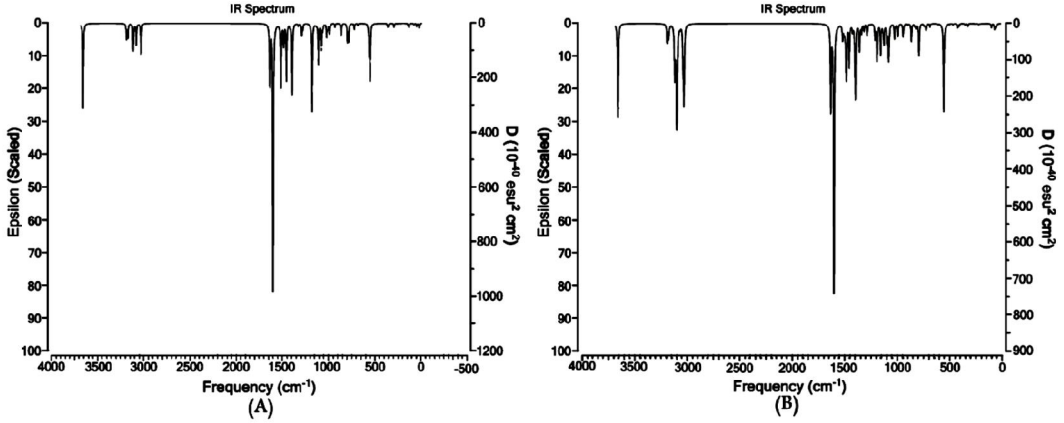

Fig. 8. IR spectra of **1** (A) and **2** (B): Calculated at B3LYP/6-311G(d,p) freq

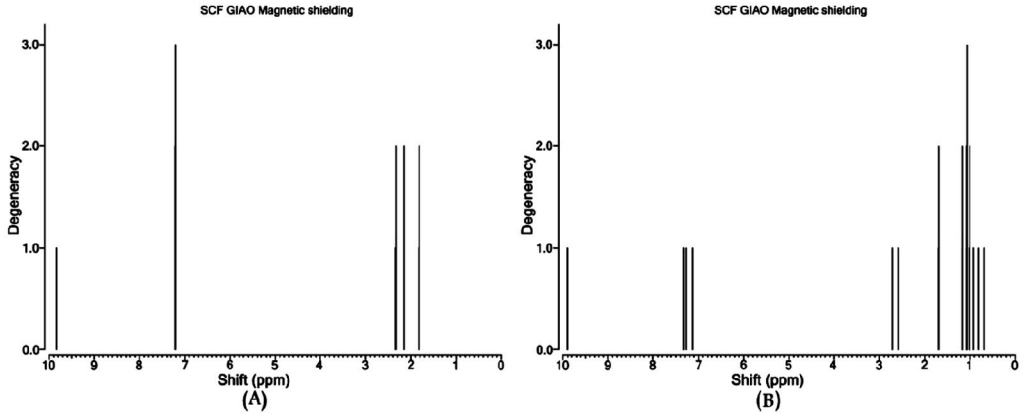

Fig. 9. Calculated ^{1}H NMR spectra of **1** (A) and **2** (B): Calculated at B3LYP/6-311 G(d, p)

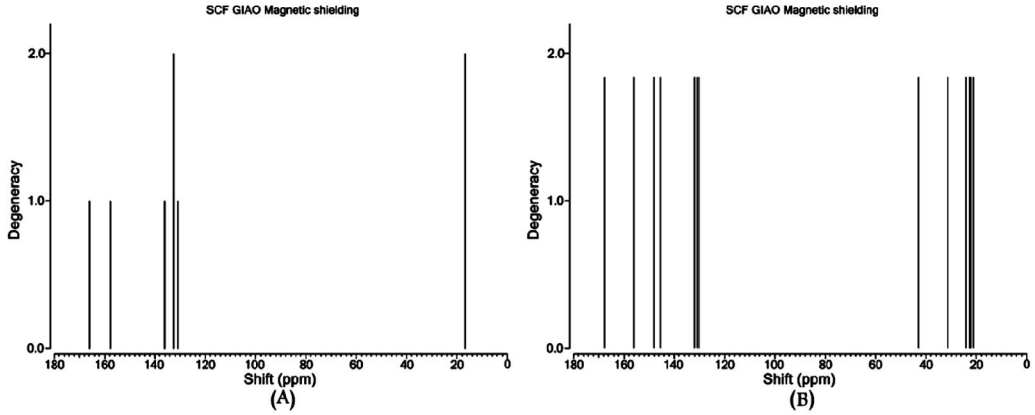

Fig. 10. Calculated ^{13}C NMR spectra of **1** (A) and **2** (B): Calculated at B3LYP/6-311 G(d,p)

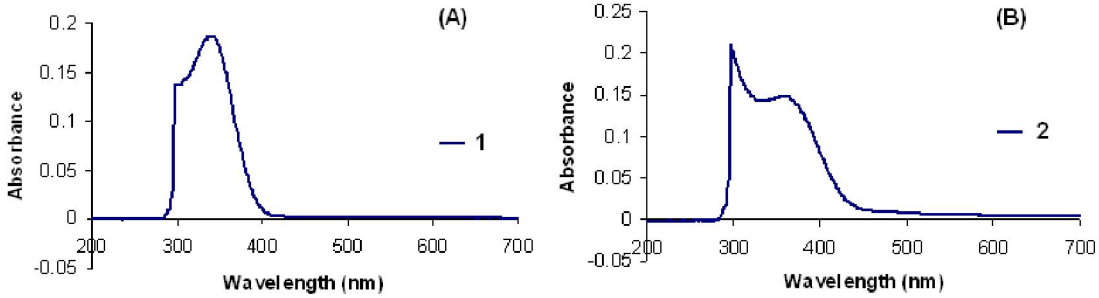

Fig. 11. UV-visible spectra of **1** (A) and **2** (B) in EtOH

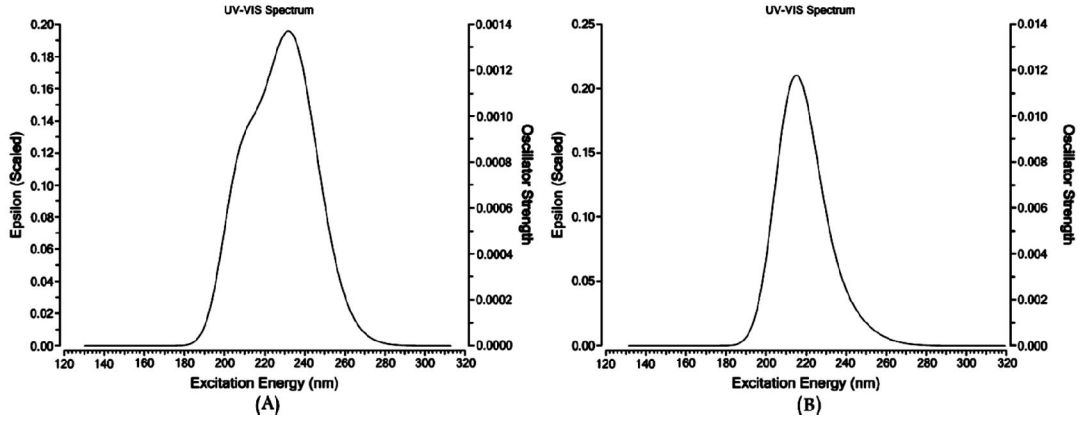

Fig. 12. Calculated UV-visible spectra of **1** (A) and **2** (B): Calculated at B3LYP/6-311 G(d,p)

The molecular geometry of compounds **1** and **2** were optimized by the calculation at DFT (B3LYP) at 6-311G(d,p) basis sets. These have been identified to correspond to local minima with all positive values of vibrational frequencies (NIMAG=0) and are shown in **Figs. 13-16**. In **1**, the rotational energy barrier for dihedral angles (φ) to rotate 360° around the bond between O1–C1 and/or O1–C2 were calculated by B3LYP/6-311G(d,p) method and equal to 7.0 kcal/mol and is shown in **Fig. 13**. And the rotational energy barrier for dihedral angles (φ) to rotate 360° around the bond between C3-C9 and/or C7-C8 were calculated by B3LYP/6-311G(d,p) method and equal to 0.9 kcal/mol and is shown in **Fig. 14**. In **2**, the rotational energy barrier for dihedral angles (φ) to rotate

360° around the bond between O1–C2 and/or O1–C7 were calculated by B3LYP/6-311G(d,p) method and equal to 13.1 kcal/mol and is shown in **Fig. 15**. And the rotational energy barrier for dihedral angles (φ) to rotate 360° around the bond between C8-C9 and/or C15-C16 were calculated by B3LYP/6- 311G(d,p) method and equal to 8.5 kcal/mol and is shown in **Fig. 16**. The corresponding maximum and minimum energies derived from rotational barrier between tetrazole – phenyl rings in **1** and **2**, between methyl - phenyl in **1** and isopropyl - phenyl ring in **2** were calculated, respectively and are summarized in **Table 4**.

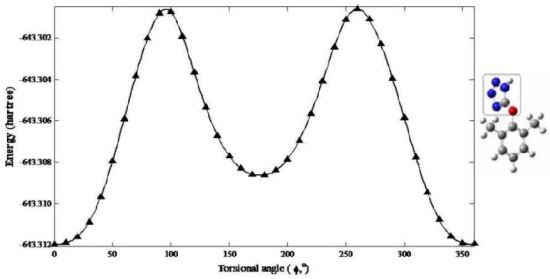

Fig. 13. Diagram of rotational energy barriers around the bond between C1-O1 and/or O1–C2 in optimized structures of **1**. Calculated at B3LYP/6-311G(d,p) level of theory

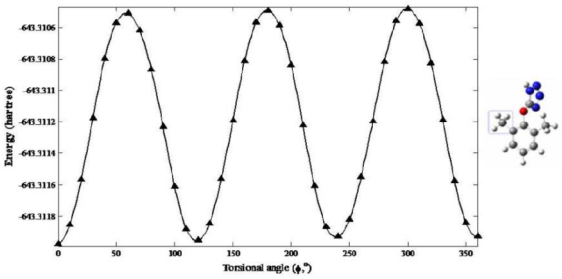

Fig. 14. Diagram of rotational barriers around the bond between C3-C9 and/or C7–C8 in optimized structures of **1**. Calculated at B3LYP/6-311G(d,p) level of theory

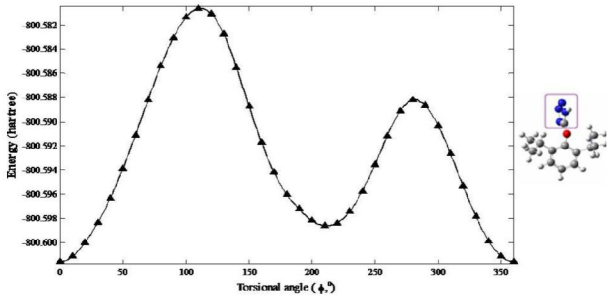

Fig. 15. Diagram of rotational barriers around the bond between C2-O1 and/or O1–C7 in optimized structures of **2**. Calculated at B3LYP/6-311G(d,p) level of theory

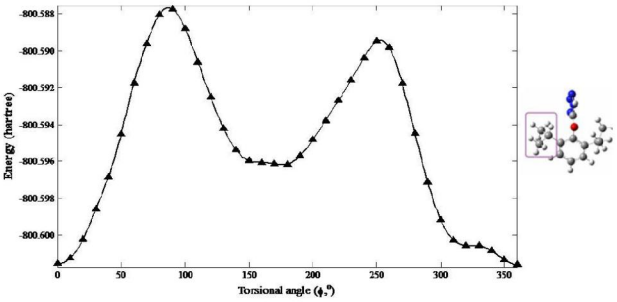

Fig. 16. Diagram of rotational barriers around the bond between C8-C9 and/or C15–C16 in optimized structures of **2**. Calculated at B3LYP/6-311G(d,p) level of theory

Table 1. Summary of crystallographic data for **1** and **2**

Crystal data (**1**)		*Crystal data* (**2**)	
Emprical Formula	$C_9H_{10}N_4O$	Emprical Formula	$C_{13}H_{18}N_4O$
M	190.21	*M*	246.31
T	293(2) K	*T*	150 K
Space group	P 2_1/c	*Space group*	P 2_1/c
a (Å)	7.589(5)	*a* (Å)	8.43778(15)
b (Å)	13.403(5)	*b* (Å)	17.5321(2)
c (Å)	9.817(5)	*c* (Å)	9.72752(16)
α (°)	90	α (°)	90
β (°)	93.028(5)	β (°)	105.1491(19)
γ (°)	90	γ (°)	90
V (Å^3)	997.146	*V* (Å^3)	1389.01 (4)
Z	4	*Z*	4
F(000)	400	*F*(000)	528
D_x (mg m^{-3})	1.267	D_x (mg m^{-3})	1.178
λ (Å)	0.71073(Mo K/α)	λ (Å)	1.54184(Cu K/α)
μ(mm^{-1})	0.089	μ(mm^{-1})	0.63
Data collection		*Data collection*	
R_{int}	0.075	R_{int}	0.025
θ_{max}	26.4°	θ_{max}	71.3°
θ_{min}	2.6°	θ_{min}	5.1°
Refinement		*Refinement*	
$R[F^2 > 2\sigma(F^2)]$	0.075	$R[F^2 > 2\sigma(F^2)]$	0.041
$wR(F^2)$	0.274	$wR(F^2)$	0.106
S	1.067	*S*	0.994

Table 2. Selected bond lengths (Å), angles (°) and torsion angles (φ) for **1** and **2**. Experimental and calculated at B3LYP/6-311G(d,p)

	Compd. **1**			Compd. **2**	
Atom	Ex.	Calcd.	Atom	Ex.	Calcd.
O1-C1	1.322	1.330	O1-C2	1.327	1.329
O1-C2	1.399	1.419	O1-C7	1.426	1.422
C1-N1	1.327	1.346	C2-N3	1.327	1.347
C1-N4	1.305	1.310	C2-N6	1.314	1.310
N1-N2	1.354	1.361	N3-N4	1.358	1.361
N1-H1	0.861	1	N3-H31	0.926	1.008
N2-N3	1.285	1.282	N4-N5	1.288	1.282
N3-N4	1.368	1.368	N5-N6	1.373	1.368
C2-C3	1.349	1.393	C7-C8	1.392	1.400
C2-C7	1.389	1.393	C7-C15	1.389	1.397
C3-C9	1.518	1.506	C8-C9	1.521	1.525
C7-C8	1.495	1.506	C15-C16	1.528	1.523
C1-O1-C2	117.3	118.01	C2-O1-C7	114.49	118.63
O1-C1-N1	121.0	120.74	O1-C2-N3	121.3	120.38
O1-C1-N4	129.3	130.03	O1-C2-N6	128.5	130.50
C1-N1-H1	126.1	130.36	C2-N3-H31	129	130.32
O1-C2-C3	117.8	117.87	O1-C7-C8	116.8	117.12
O1-C2-C7	116.3	117.87	O1-C7-C15	117.9	118.79
C2-C3-C9	120.4	121.25	C7-C8-C9	120.8	124.61
-	-	-	C8-C9-H91	106.1	104.83
-	-	-	C10-C9-C11	111.7	111.69
C2-C7-C8	123.0	121.23	C7-C15-C16	122.2	123.01
-	-	-	C15-C16-H161	106.3	108.116
-	-	-	C17-C16-C18	111.1	111.47
C2-O1-C1-N1	170.0	179.95	C7-O1-C2-N3	-174.8	-178.97
O1-C1-N1-H1	-0.8	0.04	O1-C2-N3-H31	-7.5	0.24
O1-C2-C3-C9	4.4	-4.82	O1-C7-C8-C9	1.5	1.16
O1-C2-C3-C4	-175.4	175.69	O1-C7-C8-C12	-176.5	-177.4
O1-C2-C7-C8	-5.7	4.86	O1-C7-C15-C16	-2.0	-1.59
-	-	-	C7-C8-C9-C10	154.1	119.45
-	-	-	C7-C8-C9-C11	-80.2	-63.94
-	-	-	C7-C15-C16-C17	-110.7	-116.06
-	-	-	C7-C15-C16-C18	124.2	118.73

Table 3. Hydrogen-bond geometry of **1** and **2** (Å, °)

	D-H···A	D-H (Å)	H···A (Å)	D···A (Å)	D-H···A (degree, °)
Exp.[a] (**1**)	N1-H1···N4[b]	0.861	1.959	2.804	166.9
Calcd.[c] (**1**)	N21-H24···N44	1.015	1.863	2.869	170.66
Exp.[a] (**2**)	N3-H31···N6[d]	0.926	1.919	2.835	169.1
Calcd.[c] (**2**)	N17-H20···N54	1.009	1.938	2.940	171.46

[a] Experimental
[b] Symmetry codes: (i) *x*, −*y*+3/2, *z*+1/2
[c] Calculated at B3LYP/6-311G(d,p)
[d] Symmetry codes: (i) *x*, −*y*+3/2, *z*+1/2

Table 4. Calculated maximum and minimum energies derived from rotational barrier between tetrazole and phenyl rings in **1** and **2** (B3LYP/6-311G(d,p))

Compd.	Rotation		Degree (°)	Rotational barrier (kcal/mol)
1	Tet.-Ph	Max.[a]	90-100, 255-265	7.0
		Min.[b]	-	-
	Me-Ph	Max.	55-65, 175-185, 295-305	0.9
		Min	-	-
2	Tet.-Ph	Max.	105-115	13.1
		Min.	275-285	6.5
	iso-pr.-Ph	Max.	85-95	8.5
		Min.	245-255	4.1

[a] Maximum
[b] Minimum

2.1. Computational details

All the calculations were performed with GAUSSIAN-03 packages [18]. Molecular geometries was calculated at B3LYP/6-311G(d,p) level [19-23]. Chemical shifts δi were calculated by subtracting the appropriate isotropic part σi of the shielding tensor from that of standard compound $\delta i = \sigma st - \sigma i$ (ppm). The standards TMS were calculated using the same methods and basis set. The following calculated isotropic shielding constants for TMS were obtained: 31.88 (ppm) for ^{1}H nuclei and 182.47 (ppm) for ^{13}C nuclei at B3LYP/6-311G(d) level.

2.2. Crystallographic data

For the crystal structure determination, the single-crystal of the compound **1** was used for data collection on a four-circle Rigaku R-AXIS RAPID-S diffractometer (equipped with a two dimensional area IP detector). The graphite-monochromatized MoKα radiation (λ = 0.71073 Å) and oscillation scans technique with Δω=5˚ for one image were used for data collection. The lattice parameters were determined by the least-squares methods on the basis of all reflections with F2>2σ(F2). Integration of the intensities, correction for Lorentz and polarization effects and cell refinement was performed using *Crystal Clear* (Rigaku/MSC Inc., 2005) software [24]. The structures were solved by direct methods using *SHELXS-97* [25] and refined by a full-matrix least-squares procedure using the program *SHELXL-97* [25]. The crystal structures of **1** and **2** and their crystal packing diagrams are shown in **Fig. 1** and **Fig. 2**, respectively. Some of the crystallographic data of **1** and **2** are given in **Table 1**. The selected bond lengths, angles and torsion angles with their calculated data for **1** and **2** are shown in **Table 2**. For the crystal structure determinations, single-crystals of **2** were used for data collection on an Oxford Diffraction Gemini E diffractometer. The computing details; Data collection: Gemini, (Oxford Diffraction, 2006) [26]; cell refinement: *CrysAlis RED*, (Oxford Diffraction, 2006) [26]; data reduction: *CrysAlis RED*, (Oxford Diffraction, 2002) [26]; program(s) used to solve structure: *SIR92* [27]; program(s) used to refine structure: *CRYSTALS* [28]; molecular graphics: *CAMERON* [29]; software used to prepare material for publication: *CRYSTALS* [28]. The crystallographic data for structures **1** (entry no. CCDC-838541) and **2** (entry no. CCDC-819010) were deposited to the Cambridge Crystallographic Data Center and are available free of charge upon request to CCDC, 12 Union Road, Cambridge, UK (Fax: +44-1223-336033, *e-mail*: deposit@ccdc.cam.ac.uk).

3. Conclusion

In summary, the structures of 5-(2,6-dimethylphenoxy)-(1*H*)-tetrazole **1** and 5-(2,6-diisopropylphenoxy)-(1*H*)-tetrazole **2** were elucidated by X-ray crystallography. The crystal packing diagrams of these compounds exhibits an intermolecular N1–H1···N4 and N3– H31···N6 hydrogen bonds, respectively and compared with those calculated by B3LYP/6-311G(d,p) method. These structures were also analyzed at B3LYP/6-311G(d,p) method in the gas phase. The N1-H1 and N3–H31 form of tetrazoles were found to be more stable in both solid and gas phases. IR, ^{1}H, ^{13}C NMR and UV-visible spectra were calculated at B3LYP/6-311G(d,p) method and were in good agreement with the corresponding experimental results. The rotational barrier around between phenyl and tetrazole rings and also between phenyl ring and isopropyl group in **2** is higher than that of rotational barrier in **1**.

Acknowledgements

This work was supported by the Urmia University Research Council.

4. Experimental

4.1. Instruments and materials

The ^{1}H and ^{13}C NMR spectra of **1** and **2** were recorded on Bruker 300 FT-NMR at 300 and 75 MHz for ^{1}H and ^{13}C NMR, respectively (Urmia University, Urmia, Iran). ^{1}H and ^{13}C NMR spectra were obtained on solution in DMSO-d_6 as solvent using TMS as internal standard. UV-visible spectra were measured in ethanol on a T80UV-visible (PG instrument Ltd.) spectrometer (Urmia University, Urmia, Iran). The FT-IR spectrum of **1** and **2** were determined in the region 4000- 400 cm^{-1} on a NEXUS 670 FT IR spectrometer by preparing KBr pellets (Urmia University, Urmia, Iran).

4.2. Synthesis

Tetrazoles **1** and **2** were synthesized based on reported literatures [14]. Representatively, for the synthesis of **2**, in a 50 ml round bottom flask equipped with an ice-bath and magnetically stirrer dissolved 0.127 g (1.2 mmol) BrCN in 5 ml acetone then the solution of dissolved 0.178 g (1.0 mmol) 2,6-diisopropylphenol and 0.152 g (1.5 mmol, 0.21 ml) Et_3N in acetone added drop wise into the flask by separatory funnel and stirred for 5 h at 0 °C to room temperature. The white precipitate was filtered off and was washed with few ml of dry acetone. Then the liquid residue was transferred into a separatory funnel and added drop wise into a solution of 0.10 g (1.5 mmol) NaN_3 in 5 ml water in a round bottom flask, stirred and refluxed for 1 h. The residue acetone evaporated under reduced pressure. After cooling, the solution was acidified by HCl (conc.) in an ice-bath, buff color solid was precipitated, filtered off and washed with few ml mixture of methanol and water then dried and recrystallized in chloroform: cyclohexane. Yield 70%, mp 132-133 °C. FT-IR (KBr), ν, cm^{-1}: 2455-3450 (NH), 1599 (C=C), 1570 (C=C), 1449 (*iso*-pr. bend.), 1053 (C-O). ^{1}H NMR (300 MHz, DMSO-d_6), δ: 1.08 (d, 6H, J = 6.3 Hz), 2.90 (sept., 1H, J = 6.3 Hz), 7.25 (m, 3H). ^{13}C NMR (75 MHz, DMSO-d_6), δ: 167.6, 148.4, 140.4, 127.6, 125.0, 27.1, 23.3.

Supplementary data

Full experimental and calculated data for tetrazoles **1** and **2** were available.

References

1. Demarinis R. M., Hoover J. R. E., Dunn G. L., Actor P., Uri J. V. and Weisbach J. A. (1975) A new parentral cephalosporin, SK&F-59962; 7-trifuoromethylthioacetamido-3-(1-methyl-1*H*-tetrazole-5-yl)-3-cephem-4-carboxylic acid. Chemistry and structure activity relationships. *J. Antibiot.* 28, 463-465
2. Upadhayaya R. S., Jain S., Sinha N., Kishore N., Chandra R. and Arora S. K. (2004) Synthesis of novel substituted tetrazoles having antifungal activity. *Eur. J. Med. Chem.,* 39, 579-592.
3. Witkowski J. K., Robins R. K., Sidwell R. W. and Simon L. N. (1972) Design, synthesis, and broad spectrum antiviral activity of 1-beta-D-ribofuranosyl-1,2,4-triazole-3-carboxamide and related nucleosides. *J. Med. Chem.*, 15, 1150-1154.
4. Maxwell J. R., Wasdahl D. A., Wolfson A. C. and Stenberg V. I. (1984) Synthesis of 5-aryl-2*H*-tetrazoles, 5-aryl-2*H*-tetrazole-2-acetic acids, and [(4-phenyl-5-aryl-4*H*-1,2,4-triazol-3-yl)thio]acetic acids as possible superoxide scavengers and antiinflammatory agents. *J. Med. Chem.*, 27,1565-1570
5. Lee K. H., Park C.-E., Min K.-H., Shin Y.-J., Chung C.-M., Kim H.-H., Yoon H.-J., Kim W., Ryu E.-J., Shin Y.-J., Nam H.-S., Cho J.-W. and Lee H.-Y. (2010) Synthesis and pharmacological evaluation of 3-aryl-3-azolylpropan-1-amines as selective triple serotonin/norepinephrine/dopamine reuptake inhibitors. *Bioorg. Med. Chem. Lett.*, 20, 5567-5571.

6. Pande K., Tandon M., Bhalla T. N., Parmar S. S. and Barthwal J. P. (1987) Tetrazoles as potent anti-inflammatory agents. *Pharmacology*, 35, 333-338.
7. Terashima K., Tanimura T., Shimamura H., Kawase A., Uenishi K., Tanaka Y., Kamisaki I., Ishizuka Y. and Sato M. (1995) Studies on antiulcer agents. II. Antiulcer properties of *N*-(1*H*-Tetrazol-5-yl)-2-anilino-5-pyrimidinecarboxamides inhibiting release of histamine from passively sensitized rat peritoneal mast cells. *Chem. Pharm. Bull.*, 43, 1042-1044.
8. Hayao S., Havera H. J., Strycker W. G., Leipzig T. J. and Rodriguez R. (1965) New antihypertensive aminoalkyltetrazoles. *J. Med. Chem.*, 10, 400-402.
9. Palazzi A., Stagni S., Selva S. and Monari M. (2003) Synthesis and reactivity of a new Fe(II) 5-(4-pyridyl)-tetrazolate complex and X-ray structure of its doubly protonated derivative. *J. Organometall. Chem.*, 669, 135-140.
10. Herbst R. M. and Groff S. (Eds), (1956) *Essays in Biochemistry*, John & Wiley, NewYork.
11. Moderhack D. (1988) Ring transformations in tetrazole chemistry. *J. Prakt. Chem.*, 340, 687-709.
12. Hiskey M., Chavez D. E., Naud D. L., Son S. F., Berghout H. L. and Bome C. A. (2000) Progress in high-nitrogen chemistry in explosives, propellants and pyrotechnics. *Proc. Int. Pyrotech. Semin.*, 27, 3-14.
13. Li J., Ren T., Liu H., Wang D. and Liu W. (2000) The tribological study of a tetrazole derivative as additive in liquid paraffin. *Wear*, 246, 130-133.
14. Dabbagh H. A. and Lwowski W. (2000) Equilibria of the 5-substituted-1,2-acylated tetrazoles and imidoyl azides. *J. Org. Chem.*, 65, 7284-7290.
15. Butler R. N. in Katritzky A. R., Ress C. W. and Scriven E. F. V. (Eds.) (1996) "*comprehensive heterocyclic chemistry*", vol. 4, Pergamon, Oxford, U.K., p. 621.
16. Butler R. N. in Katritzky A. R. and Boutton A. J. (Eds.) (1977) "*Advances in heterocyclic chemistry*", vol. 21, Academic Press, New York.
17. Sasaki T., Kanematsu M. and Murata M. (1971) Tetrazolo-azido isomerization in heteroaromatics—II : Syntheses and chemical reactivities of tetrazolopyridines. *Tetrahedron*, 27, 5121-5129.
18. Frisch M. J., Trucks G. W., Schlegel H. B., Scuseria G. E., Robb M. A., Cheeseman J. R., Montgomery J. A. Jr., Vreven T., Kudin K. N., Burant J. C., Millam J. M., Iyengar S. S., Tomasi J., Barone V., Mennucci B., Cossi M., Scalmani G., Rega N., Petersson G. A., Nakatsuji H., Hada M., Ehara M., Toyota K., Fukuda R., Hasegawa J., Ishida M., Nakajima T., Honda Y., Kitao O., Nakai H., Klene M., Li X., Knox J. E., Hratchian H. P., Cross J. B., Adamo C., Jaramillo J., Gomperts R., Stratmann R. E., Yazyev O., Austin A. J., Cammi R., Pomelli C., Ochterski J. W., Ayala P. Y., Morokuma K., Voth G. A., Salvador P., Dannenberg J. J., Zakrzewski V. G., Dapprich S., Daniels A. D., Strain M. C., Farkas O., Malick D. K., Rabuck A. D., Raghavachari K., Foresman J. B., Ortiz J. V., Cui Q., Baboul A. G., Clifford S., Cioslowski J., Stefanov B. B., Liu G., Liashenko A., Piskortz P., Komaromi I., Martin R. L., Fox D. J., Keith T., Al-Laham M. A., Peng C. Y., Nanayakkara A., Challacombe M., Gill P. M. W., Johnson B., Chen W., Wong M. W., Gonzalez C., Pople J. A. (2004) Gaussian 03, revision D.01. Gaussian Inc., Wallingford, CT.
19. Lee C., Yang W. and Parr R. G. (1988) Development of the Colle-Salvetti correlation-energy formula into a functional of the electron density. *Phys. Rev.*, B37, 785-789.
20. Becke A. D. (1993) A new mixing of Hartree–Fock and local density-functional theories. *J. Chem. Phys.*, 98, 1372-1377.
21. Stephens P. J., Devlin F. J., Chabalowski C. F. and Frisch M. J. (1994) Ab initio calculation of vibrational absorption and circular dichroism spectra using density functional force fields. *J. Phys. Chem.*, 98, 11623-11627.
22. Hariharan P. C. and Pople J. A. (1973) The influence of polarization functions on molecular orbital hydrogenation energies. *Theoret. Chimica Acta*, 28, 213-222.
23. Francl M. M., Petro W. J., Hehre W. J., Binkley J. S., Gordon M. S., DeFrees D. J. and Pople J. A. (1982) Self-consistent molecular orbital methods. XXIII. A polarization-type basis set for second-row elements. *J. Chem. Phys.* 77, 3654-3665.
24. Rigaku/MSC, Inc., 9009 new Trails Drive, The Woodlands, TX 77381.

25. Sheldrick G. M. (1997) *SHELXS97* and *SHELXL97*, University of Göttingen, Germany.
26. Oxford Diffraction (2006) CrysAlis CCD, CrysAlis RED and CrysAlis PRO. Oxford Diffraction Ltd, Abingdon, England.
27. Altomare A., Cascarano G., Giacovazzo C., Guagliardi A., Burla M. C., Polidori G. and Camalli M. (1994) *SIR*92 - a program for automatic solution of crystal structures by direct methods. *J. Appl. Cryst.*, 27, 435-436.
28. Betteridge P. W., Carruthers J. R., Cooper R. I., Prout K. and Watkin D. J. (2003) *CRYSTALS* version 12: software for guided crystal structure analysis. *J. Appl. Cryst.*, 36, 1487.
29. Watkin D. J., Prout C. K. and Pearce L. J. (1996) *CAMERON*, Chemical Crystallography Laboratory, Oxford, UK.